**Biophysical Journal, Volume *111***

## Supplemental Information

# Measuring Cell Viscoelastic Properties Using a Microfluidic Extensional Flow Device

**Lionel Guillou, Joanna B. Dahl, Jung-Ming G. Lin, AbduI I. Barakat, Julien Husson, Susan J. Muller, and Sanjay Kumar**

**Measuring cell viscoelastic properties using a microfluidic extensional flow device**

L Guillou[†], JB Dahl[†], JM Lin[†], AI Barakat, J Husson, SJ Muller, S Kumar[*]

†These authors contributed equally to this work
*Corresponding author

## SUPPORTING MATERIAL

### *SUPPORTING RESULTS*

*Derivation of the normalized entrance velocity ξ that best matches experimental measurements*

Experimental values for $\xi$ will lie between $\xi_{min}$ and $\xi_{max}$, provided that we restrict our analysis to objects that are near the center of the channel. In such instances, the objects will be spread in the vertical axis between the heights r and h-r, where r is the radius of the spherical object. Indeed, it is not possible for a spherical object's center to get closer to the channel walls than r. We show an example in Figure 1B (dotted black line) where r = h/16, corresponding to an experimental case in which the channel height is 200 μm and the object's radius is at least 25 μm. To obtain those $\xi$ values, we take the mean velocity along the heights considered using the velocity profile provided in Ref. (26). We find using these formulas that for our devices and objects (both dextran beads and cells), the analytical values for $\xi$ are close to 1.5 (between 1.48 and 1.62). We also experimentally measure object velocities in the cross-slot, and find that they are about 1.5 times the mean velocity in the channel. Therefore, for simplicity, we use the value $\xi = 1.5$ in our experimental analysis.

*Cells do not perturb the flow sufficiently to modify the strain rate in the device*

For the calculations of strain rate in the cross-slot, it is assumed that the flow field is unaffected by suspended cells. To determine if the presence of cells in the fluid flow affects the fluid velocity and gradients, we inspect the Stokes number of the suspended cells, which is the ratio of particle momentum relaxation time (i.e. exponential decay of particle velocity due to drag) to the characteristic time scale of the continuum fluid phase. For neutrally buoyant particles with a small particle Reynolds number ($Re_p = Re(d_p^2/D^2) = \rho U d_p^2/(\mu D) < 0.013$), the momentum relaxation time scale is independent of density and can be expressed as $\tau_{mom} = d_p^2/(18\nu_c)$ where $\nu_c = \mu_c/\rho_c$ is the kinematic viscosity of the continuum fluid phase and $d_p$ the diameter of the dispersed particles. Cells with a typical diameter of 10 μm and suspended in 20% w/v PEG20000/PBS ($\rho_c \sim 1040$ kg/m$^3$, $\mu_c \sim 0.04$ Pa·s) thus have a momentum relaxation time of $\tau_{mom} = 1.4 \cdot 10^{-7}$ seconds. The characteristic flow time scale is taken to be the inverse of the velocity gradient in the cross-slot region, $\Omega$. The smallest strain rate in our cell cross-slot experiments is $\Omega = 34$ s$^{-1}$, leading to a maximum characteristic flow field time scale of $\tau_{flow} = 2.9 \cdot 10^{-2}$ seconds. Thus, the Stokes number for our cell cross-slot experiments $Stk = \tau_{mom}/\tau_{flow} = 5 \cdot 10^{-6} << 1$. Thus, the suspended cells follow the flow field streamlines instantaneously, and the strain rate in a cross-slot device $\Omega$ is undisturbed by the presence of the cells.

*Uncertainty in cell strain measurements: User bias and small strains*

We verified that the manual strain measurement was accurate within 2% strain by having different individuals analyze the same set of cells and set of cross-slot experiments (Supporting Figure S3). Observed cell strains were small at the lower strain rates, so that the difference in length of the major and minor axes was close to 1 pixel. We mitigated the limitation of resolving small deformations by measuring several cells per data point ($10 \leq n \leq 30$), which resulted in a clear trend of increasing strain with increasing strain rate for both cell types and all pharmacological conditions.

*Viscous forces acting on cell surface in planar extensional flow*

The suspending fluid that is considered to be a Newtonian fluid has a Cauchy stress tensor of the form $\mathbf{T} = -\text{grad}(p) + \mu(\text{grad}(\mathbf{v}) + \text{grad}(\mathbf{v})^T)$ where p is the fluid pressure, $\mu$ the dynamic viscosity, and $\mathbf{v}$ the fluid velocity. Assume that the perturbations to the fluid velocity field due the presence of the cell are small, which is reasonable for our system as argued above. Due to the uniform velocity gradient in planar extensional flow $\text{grad}(\mathbf{v}) = [-\Omega\ 0\ 0;\ 0\ \Omega\ 0;\ 0\ 0\ 0]$ where $\Omega$ is the extensional strain rate, the viscous contribution to the fluid stress tensor is independent of location in the extensional flow field. Therefore, the force from the fluid (traction vector $\mathbf{t} = \mathbf{Tn}$) acting on the cell surface only depends on the local outward unit normal vector $\mathbf{n}$ of the cell surface. The viscous force vectors on the equator of a sphere and ellipsoid located anywhere in planar extensional flow, not just the stagnation point, are shown in Supporting Figure S7. The magnitude of each fluid force vector is proportional to $\mu\Omega$ and the z-component of the normal vector.

*SUPPORTING FIGURES AND TABLES*

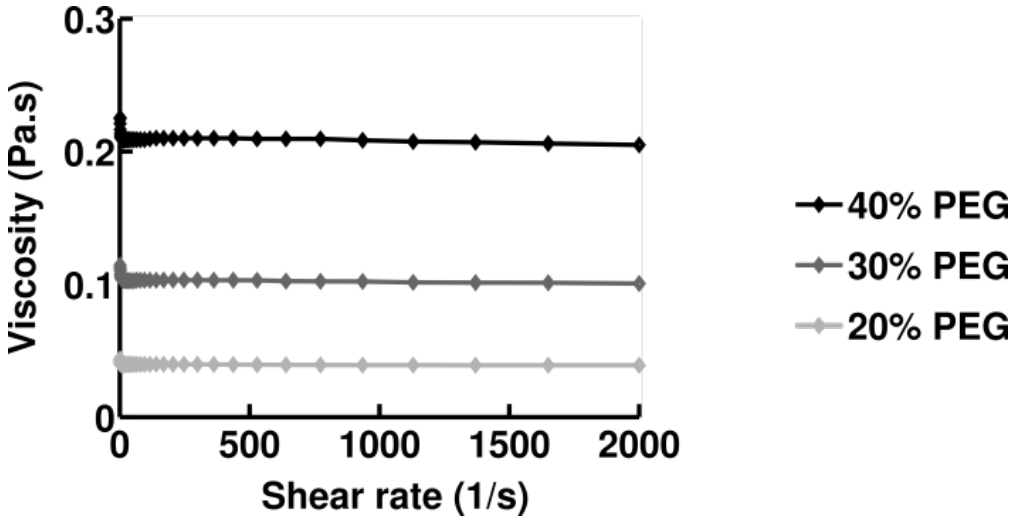


**Supporting Figure S1.** Macroscale rheologic measurements of PEG20000/PBS solutions used in cell cross-slot deformation experiments. Black line indicates 40% w/v PEG20000 in PBS, dark grey line indicates 30% w/v and light grey line 20% w/v. After initial transients at the experiment start-up, the viscosity is constant for strain rates of 1–2000 $s^{-1}$ indicating the fluid is Newtonian. The reported viscosities for each batch are the average of 2 independent rheometry measurements.

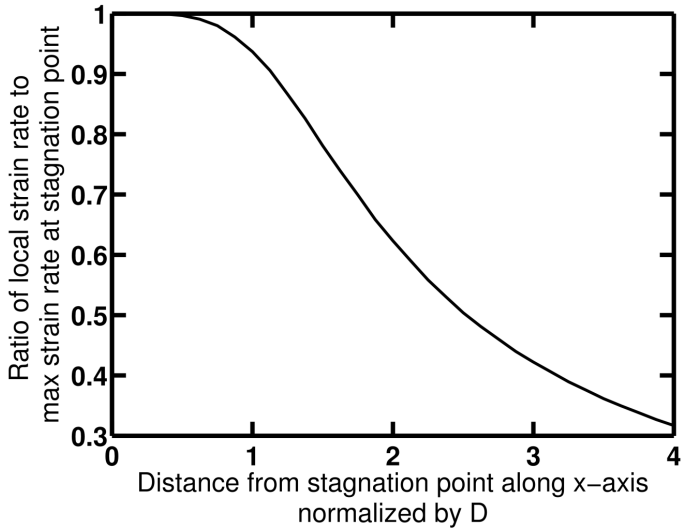


**Supporting Figure S2.** Ratio of local strain rate $\dot{\varepsilon}$ = du/dx to maximum strain rate at the cross-slot stagnation point as a function of the distance along the central inlet streamline as predicted in Hele-Shaw simulations. This streamline corresponds to the x-axis (cf. Figure 1A). The strain rate is approximately constant within a distance D (the channel half width) of the stagnation point, an

indication that the flow field is indeed hyperbolic extensional flow. Thus, objects in the stagnation point region experience a constant strain rate.

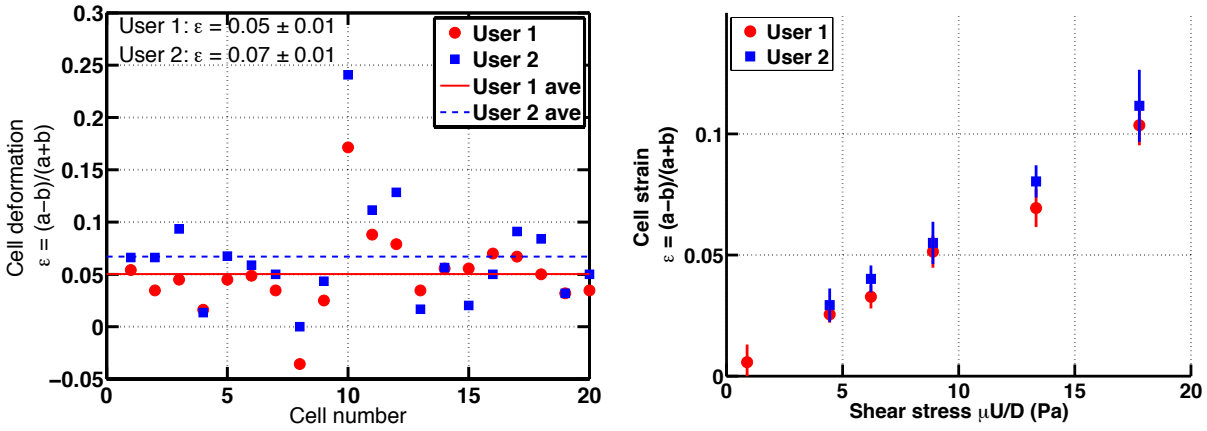


**Supporting Figure S3.** Impact of user bias on cell strain measurements is negligible. Left: Independent strain measurements performed by two users of a set of individual cells from a single cross-slot experiment (TIC control case, flow rate 300 μL/hr). Right: Independent cell strain measurements for several flow rates for control TICs by two users. Each marker is the average strain of n ≥ 10 cells and the error bars indicate ± standard error of the mean. Users independently selected qualifying cells to analyze and manually fitted ellipses in order to measure cell strain. User 2 systematically measures larger cell strain but agrees closely with User 1. For the results reported in the manuscript, User 1 performed most of the measurements.

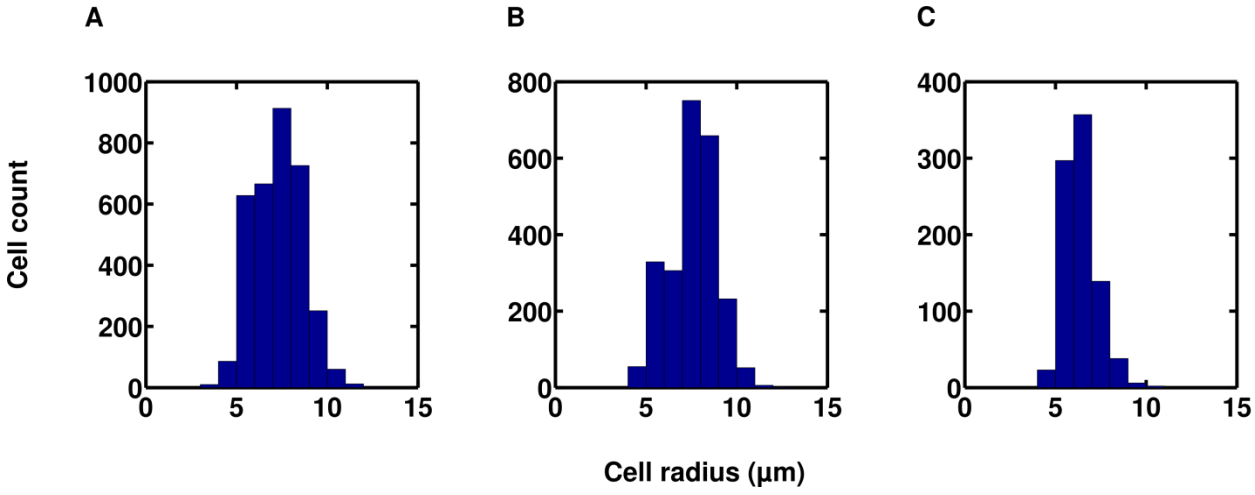


**Supporting Figure S4.** Histogram of cell radii. All analyzed cells are included. (A) Both TIC and 3T3 cells, in both control and drug conditions, are included (n = 3,357 cells). (B) Only TICs in control case are included (n = 1,288 cells). (C) Only 3T3 cells in control case are included (n = 321 cells).

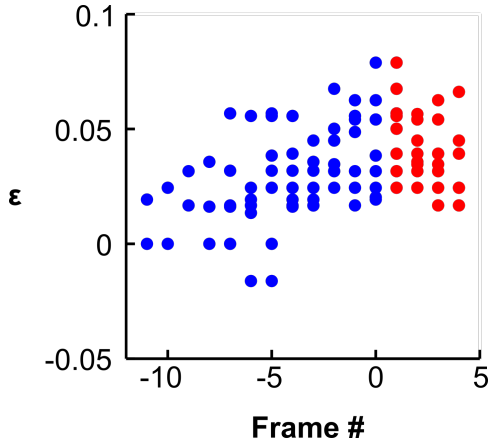


**Supporting Figure S5.** Cell deformation increases as they enter the cross-slot's central region $|\mathbf{x}| \leq D$ (blue dots), up until the point where they leave the central region and the deformation starts decreasing (red dots). Frame 0 marks the entry of the central region of the cross-slot. Cell deformation was tracked from the moment they entered the central region. Frame rate is approximately 40 fps. The cells in this example are 3T3 cells in control case at a flow rate of 250 µl/hr, with n = 8 cells tracked in this example.

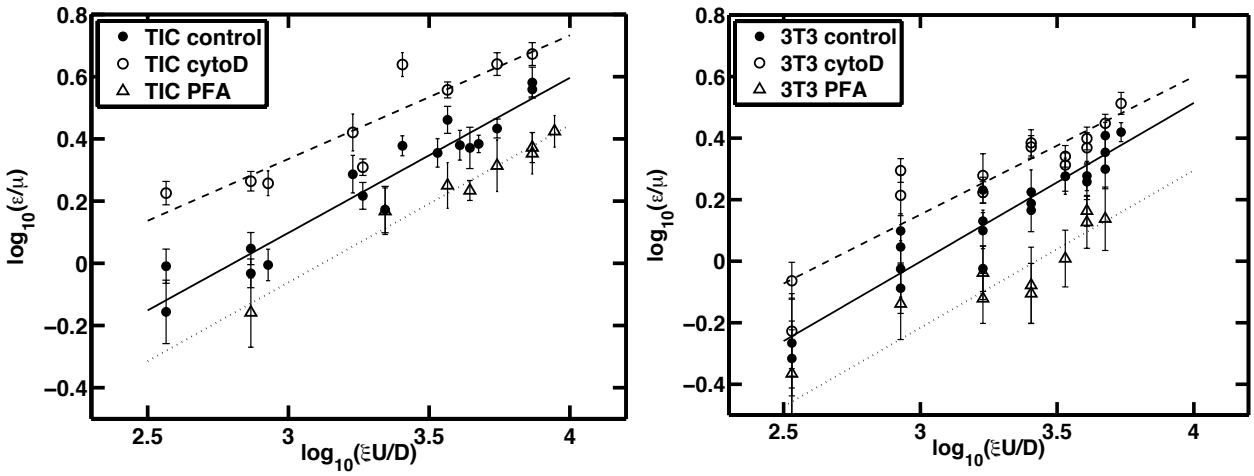


**Supporting Figure S6.** Cell cross-slot measurements including error bars reflecting the uncertainty in strain measurements (standard error of the mean). Error propagation (49) was used to plot these uncertainties for the quantity $\log(\varepsilon/\mu)$: $\sigma_{\log(\varepsilon/\mu)} = [d(\log(\varepsilon/\mu))/d\varepsilon]^2 \cdot (\sigma_\varepsilon)^2 = \sigma_\varepsilon/\varepsilon$.

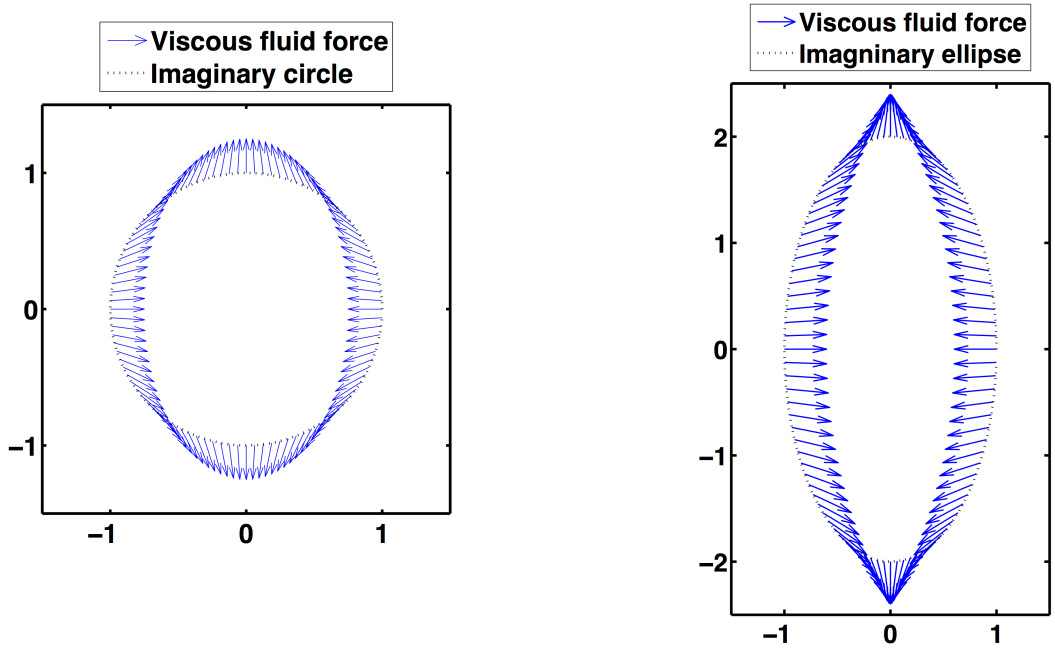


**Supporting Figure S7.** Viscous fluid forces acting on the surface of a sphere (left) and ellipsoid (right) in planar extensional flow that is unperturbed by the presence of the object. The force vectors in the x-y plane at the equator have a uniform magnitude equal to $2\mu\Omega$ ($\mu$ fluid viscosity, $\Omega$ extensional strain rate) and different directions.

**Supporting Table S1.** Range for various experimental parameters over all experimental conditions tested for the glioblastoma tumor initiating cells (TIC) and 3T3 fibroblast cells. $U = Q/(h \cdot w)$ is the average flow velocity in the channels based on the specified flow rate Q and channel cross-sectional dimensions (width $w = 2 \cdot D$, height $h = 30$ μm). The suspending fluid viscosity μ was measured before each set of experiments (sample measurements Supporting Figure S1). The flow Reynolds number Re is based on microchannel dimensions, fluid properties, and flow rate. n is the number of cells used to determine the average strain ε that makes up each data point in Figure 4(B,C).

| **Cell Type** | **μ** | **w** | **U** | **$Re = \rho UD/\mu$** | **$\xi U/D$** | **n** | **$\varepsilon = (a-b)/(a+b)$** |
|---|---|---|---|---|---|---|---|
| | [mPa·s] | [μm] | [mm/s] | | $s^{-1}$ | | |
| **TIC** | $36 \le \mu \le 42$ | w = 70, 100 | $7 \le U \le 159$ | $0.0057 \le Re \le 0.19$ | $283 \le \xi U/D \le 6800$ | $10 \le n \le 27$ | $0.029 \le \varepsilon \le 0.18$ |
| **3T3** | $37.5 \le \mu \le 38.3$ | w = 100 | $9 \le U \le 148$ | $0.013 \le Re \le 0.20$ | $278 \le \xi U/D \le 4440$ | $10 \le n \le 30$ | $0.009 \le \varepsilon \le 0.12$ |

**Supporting Table S2**. Statistical significance (p-values) of multiple regression analysis of covariance.

| Comparison Groups | 3T3 p-value | TIC p-value |
|---|---|---|
| Control vs. CytoD | 0.012 | 0.0002 |
| Control vs. PFA | 0.0094 | 0.0015 |
| CytoD vs. PFA | 0.0004 | $8.5 \cdot 10^{-6}$ |

**Supporting Table S3.** Raw data for glioblastoma tumor initiating cells (TIC) mechanical measurements. The uncertainty ($\sigma_\varepsilon$) in the average strain measurement ($\varepsilon$) at each experimental condition is the standard error of the mean.

| TIC | Fluid viscosity μ | Channel wideth w = 2·D | Mean flow velocity U | Flow Reynolds number Re = ρUD/μ | Extensional strain rate ξU/D | Number of cells n | Average strain ε = (a-b)/(a+b) | Strain uncertainty $\sigma_\varepsilon$ |
|---|---|---|---|---|---|---|---|---|
| | mPa·s | μm | mm/s | | $s^{-1}$ | | | std error of mean |
| **TIC CONTROL** | | | | | | | | |
| Day 1 | 42 | 70 | 6.61 | 0.0057 | 283 | 14 | 0.029 | 0.007 |
| | | | 13.23 | 0.0115 | 567 | 15 | 0.047 | 0.006 |
| | | | 39.68 | 0.0344 | 1701 | 12 | 0.06 | 0.01 |
| | | | 79.37 | 0.0688 | 3401 | 16 | 0.10 | 0.02 |
| | | | 132.28 | 0.1146 | 5669 | 15 | 0.16 | 0.02 |
| Day 2 | 36 | 100 | 23.15 | 0.0334 | 694 | 11 | 0.036 | 0.004 |
| | | | 46.30 | 0.0669 | 1389 | 15 | 0.07 | 0.01 |
| | | | 69.44 | 0.1003 | 2083 | 15 | 0.086 | 0.006 |
| | | | 92.59 | 0.1337 | 2778 | 15 | 0.082 | 0.009 |
| | | | 111.11 | 0.1605 | 3333 | 14 | 0.09 | 0.01 |
| | | | 129.63 | 0.1872 | 3889 | 11 | 0.087 | 0.006 |
| Day 3 | 37.6 | 70 | 6.61 | 0.0064 | 283 | 12 | 0.037 | 0.005 |
| | | | 13.23 | 0.0128 | 567 | 18 | 0.035 | 0.004 |
| | | | 33.07 | 0.0320 | 1417 | 20 | 0.062 | 0.006 |
| | | | 66.14 | 0.0640 | 2834 | 20 | 0.11 | 0.01 |
| | | | 99.21 | 0.0960 | 4252 | 27 | 0.102 | 0.007 |
| | | | 132.28 | 0.1281 | 5669 | 22 | 0.136 | 0.008 |
| **TIC CYTOCHALASIN D** | | | | | | | | |
| Day 2 | 36 | 100 | 23.15 | 0.0334 | 694 | 18 | 0.065 | 0.006 |
| | | | 46.30 | 0.0669 | 1389 | 20 | 0.09 | 0.01 |
| | | | 69.44 | 0.1003 | 2083 | 15 | 0.16 | 0.01 |
| Day 3 | 37.6 | 70 | 6.61 | 0.0064 | 283 | 14 | 0.063 | 0.005 |
| | | | 13.23 | 0.0128 | 567 | 16 | 0.069 | 0.005 |
| | | | 33.07 | 0.0320 | 1417 | 20 | 0.077 | 0.005 |
| | | | 66.14 | 0.0640 | 2834 | 20 | 0.136 | 0.008 |
| | | | 99.21 | 0.0960 | 4252 | 20 | 0.16 | 0.01 |
| | | | 132.28 | 0.1281 | 5669 | 20 | 0.18 | 0.02 |
| **TIC PFA** | | | | | | | | |
| Day 1 | 42 | 70 | 13.23 | 0.0115 | 567 | 20 | 0.029 | 0.007 |
| | | | 39.68 | 0.0344 | 1701 | 19 | 0.06 | 0.01 |
| | | | 79.37 | 0.0688 | 3401 | 18 | 0.072 | 0.005 |
| | | | 132.28 | 0.1146 | 5669 | 10 | 0.10 | 0.01 |
| Day 3 | 37.6 | 70 | 66.14 | 0.0640 | 2834 | 20 | 0.07 | 0.01 |
| | | | 99.21 | 0.0960 | 4252 | 20 | 0.08 | 0.01 |
| | | | 132.28 | 0.1281 | 5669 | 20 | 0.08 | 0.01 |
| | | | 158.73 | 0.1537 | 6803 | 20 | 0.10 | 0.01 |

**Supporting Table S4.** Raw data for 3T3 fibroblast cell mechanical measurements. The uncertainty ($\sigma_\varepsilon$) in the average strain measurement ($\varepsilon$) at each experimental condition is the standard error of the mean.

| 3T3 | Fluid viscosity μ | Channel wideth w = 2·D | Mean flow velocity U | Flow Reynolds number Re = ρUD/μ | Extensional strain rate ξU/D | Number of cells n | Average strain ε = (a-b)/(a+b) | Strain uncertainty $\sigma_\varepsilon$ |
|---|---|---|---|---|---|---|---|---|
| | mPa·s | μm | mm/s | | $s^{-1}$ | | | std error of mean |
| **3T3 CONTROL** | | | | | | | | |
| Day 1 | 37.75 | 100 | 23.15 | 0.0319 | 694 | 16 | 0.047 | 0.006 |
| | | | 46.30 | 0.0638 | 1389 | 11 | 0.047 | 0.006 |
| | | | 69.44 | 0.0957 | 2083 | 22 | 0.058 | 0.003 |
| | | | 111.11 | 0.1531 | 3333 | 15 | 0.071 | 0.008 |
| | | | 129.63 | 0.1786 | 3889 | 25 | 0.10 | 0.01 |
| | | | 148.15 | 0.2041 | 4444 | 27 | 0.099 | 0.007 |
| Day 2 | 38.3 | 100 | 23.15 | 0.0314 | 694 | 10 | 0.043 | 0.005 |
| | | | 46.30 | 0.0629 | 1389 | 10 | 0.065 | 0.006 |
| | | | 69.44 | 0.0943 | 2083 | 11 | 0.056 | 0.009 |
| | | | 92.59 | 0.1257 | 2778 | 10 | 0.072 | 0.008 |
| | | | 111.11 | 0.1509 | 3333 | 10 | 0.069 | 0.009 |
| | | | 129.63 | 0.1760 | 3889 | 19 | 0.09 | 0.01 |
| Day 3 | 37.5 | 100 | 23.15 | 0.0321 | 694 | 10 | 0.035 | 0.007 |
| | | | 46.30 | 0.0642 | 1389 | 10 | 0.051 | 0.004 |
| | | | 69.44 | 0.0963 | 2083 | 14 | 0.06 | 0.01 |
| | | | 92.59 | 0.1284 | 2778 | 13 | 0.07 | 0.01 |
| Day 4 | 37.5 | 100 | 9.26 | 0.0128 | 278 | 10 | 0.020 | 0.007 |
| | | | 23.15 | 0.0321 | 694 | 18 | 0.031 | 0.006 |
| | | | 46.30 | 0.0642 | 1389 | 10 | 0.035 | 0.006 |
| | | | 129.63 | 0.1798 | 3889 | 12 | 0.07 | 0.01 |
| **3T3 CYTO D** | | | | | | | | |
| Day 1 | 37.75 | 100 | 9.26 | 0.0128 | 278 | 21 | 0.033 | 0.005 |
| | | | 23.15 | 0.0319 | 694 | 15 | 0.074 | 0.007 |
| | | | 46.30 | 0.0638 | 1389 | 30 | 0.063 | 0.005 |
| | | | 69.44 | 0.0957 | 2083 | 12 | 0.089 | 0.008 |
| | | | 92.59 | 0.1275 | 2778 | 10 | 0.083 | 0.007 |
| | | | 111.11 | 0.1531 | 3333 | 27 | 0.095 | 0.008 |
| | | | 129.63 | 0.1786 | 3889 | 10 | 0.106 | 0.007 |
| | | | 148.15 | 0.2041 | 4444 | 20 | 0.12 | 0.01 |
| Day 2 | 38.3 | 100 | 9.26 | 0.0126 | 278 | 17 | 0.023 | 0.006 |
| | | | 23.15 | 0.0314 | 694 | 16 | 0.06 | 0.01 |
| | | | 46.30 | 0.0629 | 1389 | 12 | 0.07 | 0.01 |
| | | | 69.44 | 0.0943 | 2083 | 20 | 0.093 | 0.009 |
| | | | 92.59 | 0.1257 | 2778 | 21 | 0.079 | 0.007 |
| | | | 111.11 | 0.1509 | 3333 | 26 | 0.09 | 0.01 |
| **3T3 PFA** | | | | | | | | |
| Day 3 | 37.5 | 100 | 9.26 | 0.0128 | 278 | 15 | 0.016 | 0.005 |
| | | | 46.30 | 0.0642 | 1389 | 15 | 0.028 | 0.005 |
| | | | 69.44 | 0.0963 | 2083 | 15 | 0.031 | 0.009 |
| | | | 111.11 | 0.1541 | 3333 | 15 | 0.055 | 0.006 |
| Day 4 | 37.5 | 100 | 9.26 | 0.0128 | 278 | 11 | 0.009 | 0.005 |
| | | | 23.15 | 0.0321 | 694 | 15 | 0.027 | 0.007 |
| | | | 46.30 | 0.0642 | 1389 | 15 | 0.034 | 0.007 |
| | | | 69.44 | 0.0963 | 2083 | 15 | 0.029 | 0.007 |
| | | | 92.59 | 0.1284 | 2778 | 14 | 0.038 | 0.008 |
| | | | 111.11 | 0.1541 | 3333 | 15 | 0.05 | 0.01 |
| | | | 129.63 | 0.1798 | 3889 | 15 | 0.05 | 0.01 |